Chemosphere 81 (2010) 716–724

Contents lists available at ScienceDirect

Chemosphere

journal homepage: www.elsevier.com/locate/chemosphere

Protein profiles in zebrafish (*Danio rerio*) brains exposed to chronic microcystin-LR

Minghua Wang, Dazhi Wang *, Lin Lin, Huasheng Hong

State Key Laboratory of Marine Environmental Science/Environmental Science Research Center, Xiamen University, Xiamen 361005, People's Republic of China

ARTICLE INFO

Article history:
Received 16 March 2010
Received in revised form 20 July 2010
Accepted 28 July 2010
Available online 25 August 2010

Keywords:
Microcystin-LR
Protein phosphatase
Proteomics
Chronic toxicity

ABSTRACT

Microcystin-LR (MCLR) is a commonly encountered blue-green algal hepatotoxin and a known inhibitor of cellular protein phosphatase (PP), however, little is known about its neurotoxicity. This study investigated the protein profiles of zebrafish (*Danio rerio*) brains chronically exposed to MCLR concentrations (2 or 20 μg L^{-1}) using the proteomic approach. The results showed that MCLR strikingly enhanced toxin accumulation and the PP activity in zebrafish brains after 30 d exposure. Comparison of two-dimensional electrophoresis protein profiles of MCLR exposed and non-exposed zebrafish brains revealed that the abundance of 30 protein spots was remarkably altered in response to MCLR exposure. These proteins are involved in cytoskeleton assembly, macromolecule metabolism, oxidative stress, signal transduction, and other functions (e.g. transporting, protein degradation, apoptosis and translation), indicating that MCLR toxicity in the fish brain is complex and diverse. The chronic neurotoxicity of MCLR might initiate the PP pathway via an upregulation of PP2C in the zebrafish brain, in addition to the reactive oxygen species pathway. Additionally, the increase of vitellogenin abundance in MCLR exposed zebrafish brains suggested that MCLR might mimic the effects of endocrine disrupting chemicals. This study demonstrated that MCLR causes neurotoxicity in zebrafish at the proteomic level, which provides a new insight into MCLR toxicity in aquatic organisms and human beings.

1. Introduction

Microcystins (MCs), a group of cyclic heptapeptides, are considered to be hepatotoxins produced by a number of cyanobacterial genera. In the past few decades, MCs have become a worldwide concern due to the significant increase of MCs-producing cyanobacterial blooms in eutrophic rivers, lakes, reservoirs and recreational waters. Among 80 MCs, microcystin-LR (MCLR) is the most studied and the most toxic (Hoeger et al., 2005). The toxic effects of MCLR on fish are reported in a large number of studies including behavioral, histological, and biochemical investigations (Fischer and Dietrich, 2000; Malbrouck et al., 2003, 2004; Baganz et al., 2004; Li et al., 2007; Mezhoud et al., 2008a,b; Malécot et al., 2009; Wang et al., 2010), however most of them focus on its hepatotoxicity. Studies show that organic anion transporting polypeptides (rodent Oatp/human OATP) appear to be specifically required for the active uptake of MCs into hepatocytes (Monks et al., 2007; Feurstein et al., 2009), but Oatp/OATP are also expressed in the heart, lung, spleen, pancreas, blood–brain-barrier (BBB) and brain (Hagenbuch and Meier, 2003; Feurstein et al., 2009). Thus, regardless of their specific hepatotoxicity, MCs have been found in other organs with a concomitant display of toxicity. Fischer and Dietrich (2000) report MCLR in the brain of *Cyprinus carpio* fed with toxic algae. Cazenave et al. (2005) report the presence of microcystin-RR (MCRR) in the brain of *Jenynsia multidentata* exposed to water-dissolved toxin for 24 h. In addition to MCs in the brain of *J. multidentata*, Cazenave et al. (2008) also report changes in swimming activity of this fish upon exposure to MCs, suggesting the probable neurotoxicity of MCs. Taken together, these findings suggest that as a consequence of the high blood perfusion of the brain, significant amounts of MCs could accumulate in the brain across the BBB and result in probable neurotoxicity. Actually, the above hypothesis is supported by the tragic event occurring in Caruaru, Brazil in February 1996. Among the 131 patients intravenously exposed to various concentrations of MCs, 89% of them presented immediate signs of neurotoxicity (e.g. dizziness, tinnitus, vertigo, headache, vomiting, nausea, mild deafness, visual disturbance and blindness) with a consequent onset of overt hepatotoxicity and finally succumbed to multi-organ failure (Carmichael et al., 2001; Soares et al., 2006).

The typical toxicological action of MCs is to inhibit serine/threonine protein phosphatase (PP) (Fischer and Dietrich, 2000; Gehringer, 2004), followed by hyperphosphorylation of numerous cellular proteins, thereby resulting in the collapse of the cytoskeleton and the loss of cellular integrity (Fischer and Dietrich, 2000; Batista et al., 2003). Moreover, other toxicity mechanisms such as oxidative damage and disruption of osmoregulation are also

* Corresponding author. Tel.: +86 0592 2186016; fax: +86 0592 2186055.
E-mail address: dzwang@xmu.edu.cn (D. Wang).

0045-6535/$ - see front matter © 2010 Elsevier Ltd. All rights reserved.
doi:10.1016/j.chemosphere.2010.07.061

reported (Ding et al., 2001; Mikhailov et al., 2003; Blom and Jüttner, 2005; Chen et al., 2006). Ding et al. (2001) demonstrate that the production of reactive oxygen species (ROS) plays a crucial role in MCs-induced disruption of cytoskeleton organization and consequent hepatotoxicity. Thus, the precise mechanism of MCLR toxicity in organisms has not been well elucidated.

A large number of studies focus on the acute toxicity of MCs (Malbrouck et al., 2003, 2004; Li et al., 2007; Mezhoud et al., 2008a,b; Malécot et al., 2009), but few efforts have been devoted to exploring the chronic effects of MCs on organisms. Chronic exposure to MCs through drinking water is the main reason for toxin accumulation in organisms including human beings, considering that the concentration of MCs is usually a few micrograms per liter in the water of many eutrophic lakes in the world (Song et al., 2007; Gurbuz et al., 2009). Our previous study shows that the chronic toxicity of MCLR is different from its acute toxicity and the ROS pathway is the main toxic pathway instead of the PP one (Wang et al., 2010). So, in this study, zebrafish (*D. rerio*) were chronically exposed to MCLR (2 or 20 $\mu g\,L^{-1}$) for 30 d, the protein profiles of exposed and non-exposed zebrafish brains were analyzed using the proteomic approach, and the differentially expressed proteins were identified using MALDI-TOF/TOF MS. Toxin content and PP activity in zebrafish brains were also investigated after the 30 d exposure. Thus, we aimed to explore the chronic neurotoxicity of MCLR to zebrafish brains, and to identify potential protein biomarkers so as to understand the damage mechanisms involved.

2. Materials and methods

2.1. Zebrafish exposure experiment

Zebrafish were acclimatized in aerated fresh water tanks for 20 d prior to the experiment at a water temperature of 25 °C and a 12 h light/dark cycle, and fed twice a day, 9:00 am and 3:00 pm, with commercial dry bait. During acclimation, the fish were supplemented with artemia (about 40 mg per fish) three times a week to maintain nutritional status. Then, fish (weighing 0.7 ± 0.07 g) were randomly assigned to three experimental groups for exposure to two MCLR concentrations, 2 and 20 $\mu g\,L^{-1}$, and non-exposure. Each treatment included two groups with 40 fishes for each group. The experiments were undertaken in glass tanks ($44 \times 30 \times 28\ cm^3$) with 30 L fresh water and lasted for 30 d under the same conditions as described above during acclimation. Each day one-third of the aged water was renewed with fresh water containing 2 or 20 $\mu g\,L^{-1}$ MCLR, or none. No mortality was found in any treatment during the 30 d exposure. At the end of the experiment, zebrafish brains were dissected and pooled. Then they were immediately frozen in liquid nitrogen and stored at −80 °C for proteomic, toxin content and PP activity analysis.

2.2. MCLR analysis

MCLR content in zebrafish brains was analyzed according to the method of Moreno et al. (2005) with minor modification (Deblois et al., 2008). Briefly, freeze-dried tissue was homogenized in 0.6 mL of 85% methanol (MeOH) using an ultrasonic disrupter (Model 450, Branson Ultrasonics, Danbury, CT, USA) at 4 °C for 5 min. The homogenate was extracted at 4 °C for 6 h and then centrifuged (8000*g*) at 4 °C for 10 min, and the supernatant was recovered. The pellet was extracted again using the same procedure and the supernatant was pooled with that collected earlier and washed with the same volume of hexane for 4 h. The hexane layer was discarded and the MeOH layer was completely dried using SpeedVac. The dried brain extract was resolubilized in 100 μL of 50% MeOH for toxin analysis using HPLC with a DAD detector. The toxin separation was performed on a micropher C18 reverse phase column (3 μm) under isocratic conditions with a mobile phase of 10 mM ammonium acetate and acetonitrile (7.4:2.6) for 20 min. The toxin content was quantified using an MCLR standard and expressed as μg cellular MCLR per mg DW (dry weight).

2.3. PP activity analysis

Brain lysate was prepared using tissue protein extraction reagent (T-PER, Pierce Biotechnology Inc., Rockford, IL, USA). 0.5 mg brain tissue was sonicated in 1 mL T-PER reagent and the supernatant was recovered by centrifugation (16 000 g) at 4 °C for 20 min. PP activity was analyzed according to the method of Fontal et al. (1999). Briefly, 35 μL of brain homogenate was mixed with 5 μL of $NiCl_2$ (40 mM), 5 μL of 5 $mg\,mL^{-1}$ bovine serum albumin (Sigma) and 35 μL of phosphatase assay buffer (50 mM Tris–HCl, 0.1 mM $CaCl_2$, pH 7.4) and incubated at 37 °C for 10 min. Then 120 μL of 100 μM 6,8-difluoro-4-methylumbelliferyl phosphate (Sigma) was added and it was incubated at 37 °C for another 30 min. PP activity was analyzed using a fluorescence microplate reader at 355 nm (excitation) and 460 nm (emission).

2.4. Proteomic analysis

2.4.1. Protein extraction

Frozen fish brains were homogenized in 0.6 mL of 20% TCA/acetone (w/v) lysis buffer with 20 mM dithiothreitol (DTT) using an ultrasonic disrupter. The supernatant was removed by centrifugation at 17 000 g for 30 min at 4 °C, and the pellet was washed twice with 80% acetone (v/v) and twice with ice-cold acetone with 20 mM DTT. The pellet was recovered by centrifugation at 17 000 g for 30 min at 4 °C each time. Residual acetone was removed in a SpeedVac for about 5 min. The pellet was dissolved in 100 μL rehydration buffer containing 8 M urea, 2% CHAPS, 2.8 $mg\,mL^{-1}$ DTT, 0.5% immobilized pH gradient (IPG) buffer and a trace of bromophenol blue. The solution was centrifuged at 20 000*g* for 30 min at 15 °C and the supernatant was collected for two-dimensional electrophoresis (2-DE) analysis. The protein content was quantified using the 2-D Quant kit (GE Healthcare).

2.4.2. 2-DE analysis

One hundred and twenty micro gram of each protein sample was mixed with a rehydration buffer and then loaded onto IPG strips of linear pH gradient 4–7 (GE Healthcare). Rehydration and subsequent isoelectric focusing were conducted using the Ettan IPGphor III Isoelectric Focusing System (Amersham Biosciences, USA). Rehydration was performed overnight in a strip holder with 340 μL of rehydration buffer. After rehydration, isoelectric focusing was performed in the following manner: 2 h at 100 V, 2 h at 200 V, 1 h at 500 V, 2 h at 1000 V, 2 h at 4000 V and 6 h at 8000 V. After the first dimension was run, each strip was equilibrated with about 10 mL equilibration buffer containing 50 mM Tris (pH 8.8), 6 M urea, 30% glycerol, 2% SDS, 1% DTT and a trace amount of bromophenol blue, for 17 min. The strip was then placed in fresh equilibration buffer containing 2.5% iodoacetamide (instead of DTT) for another 17 min. Subsequently an 11.25% SDS–PAGE second dimension was performed. Electrophoresis was carried out at 10 mA/gel for 15 min, followed by a 6 h run at 200 V until the bromophenol blue front reached the edge of the gels. The proteins were visualized by silver staining and three 2-DE gels were performed for each sample. Unless stated otherwise, the 2-DE gels shown were representative of the three gels performed.

2.4.3. Silver staining

Silver staining was performed following the method of Wang et al. (2009). Briefly, the gel was fixed for 2 h initially in a fixation solution containing 40% (v/v) ethanol and 10% (v/v) acetic acid. It was then sensitized in a solution containing 30% (v/v) ethanol, 0.2% (w/v) sodium thiosulphate, 6.8% (w/v) sodium acetate and 0.125% (v/v) glutaraldehyde, followed by three Milli-Q water washes (5 min each time). Then the gel was stained for 20 min in 0.25% (w/v) silver nitrate with 0.015% (v/v) formaldehyde and washed twice with Milli-Q water (0.5 min each time). The gel was developed in 2.5% (w/v) sodium carbonate containing 0.0074% (v/v) formaldehyde. The reaction was stopped with 1.5% (w/v) ethylenediaminetetraacetic acid, disodium salt.

2.4.4. Image capture and analysis

Images were made using a Gel-documentation system on a GS-670 Imaging Densitometer from Bio-Rad (USA) and 2-DE electrophoretogram matching software. Images were saved in TIFF format before analysis. Computerized 2-DE gel analysis (spot detection, spot editing, pattern matching, database construction) was performed using the ImageMaster 2D Elite (GE Life Science, USA) and Melanie IV. There were three gels for samples from control or treated zebrafish brains. After spot detection and matching, spot intensities were normalized with total valid spot volume in order to minimize the nonexpression related variations in spot intensity and hence accurately provide semiquantitative information across different gels. Spots normalization was done by analyzing the relative volume (volume percentage). A one-way ANOVA (analysis of variance) test was used to analyze spot intensities among different groups. Only protein spots showing a significance ($P < 0.05$) and at least a 2.0-fold difference in abundance (ratio of mean normalized spot volume of treated *versus* control groups) were considered as up- or down-regulated. These protein spots of interest were selected for identification by mass spectrometry.

2.4.5. Mass spectrometric analysis

Differentially expressed protein spots in MCLR exposed and non-exposed brains were manually excised from 2-DE gels. The gel pieces were washed twice with 200 mM ammonium bicarbonate in 50% acetonitrile/water (20 min at 30 °C), then dehydrated using acetonitrile and spun dry. In gel trypsin digestion was performed by adding 10 ng μL^{-1} trypsin (Promega) in 25 mM ammonium bicarbonate overnight at 37 °C. For MALDI-TOF/TOF MS analysis, 1 μL of the digest mixture was mixed on-target with 1 μL of 100 mM α-cyano-4-hydroxy-cinnamic acid in 50% acetonitrile and 0.1% trifluoroacetic acid on the target plate before being dried and analyzed with a MALDI TOF/TOF mass spectrometer (4800 Proteomics Analyzer, Applied Biosystems). MALDI TOF MS and TOF-TOF tandem MS were performed and data were acquired in the positive MS reflector mode with a scan range from 900 to 4000 Da, and five monoisotopic precursors (S/N > 200) were selected for MS/MS analysis. For interpretation of the mass spectra, a combination of peptide mass fingerprints and peptide fragmentation patterns were used for protein identification in an NCBI nonredundant database using the Mascot search engine (www.matrixscience.com). All mass values were considered monoisotopic, and the mass tolerance was set at 75 ppm. One missed cleavage site was allowed for trypsin digestion; cysteine carbamidomethylation was assumed as a fixed modification, and methionine was assumed to be partially oxidized. Results with CI% (confidence interval%) values greater than 95% were considered to be a positive identification. The identified proteins were then matched to specific processes or functions by searching Gene Ontology (http://www.geneontology.org/).

2.5. Statistical tests

All measurements were replicated at least three times and the data were expressed as mean values ± standard deviation. Statistical analysis was carried out using one-way ANOVA or an independent-samples *t*-test to evaluate whether the means were significantly different among the groups. Significant differences were indicated at $P < 0.05$. Prior to one-way ANOVA, data were log transformed to meet ANOVA assumptions of normality and variance homoscedasticity.

3. Results

3.1. Effect of MCLR on toxin accumulation and PP activity in the zebrafish brain

The toxin content and PP activity in zebrafish brains at the end of this exposure experiment are shown in Fig. 1. No MCLR was detected in the control while MCLR significantly enhanced toxin accumulation in MCLR exposed zebrafish brains (Fig. 1A). The toxin contents were 0.030 and 0.053 μg mg^{-1} DW in the brains exposed to 2 and 20 μg L^{-1} MCLR (Fig. 1A). Namely, the treated MCLR content displayed a positively linear relationship with the ambient toxin concentration (Fig. 1A, $P < 0.05$). Similarly, the brain PP activity was also enhanced by MCLR and the PP activity increased 1.3 times in zebrafish brains exposed to 20 μg L^{-1} MCLR (Fig. 1B).

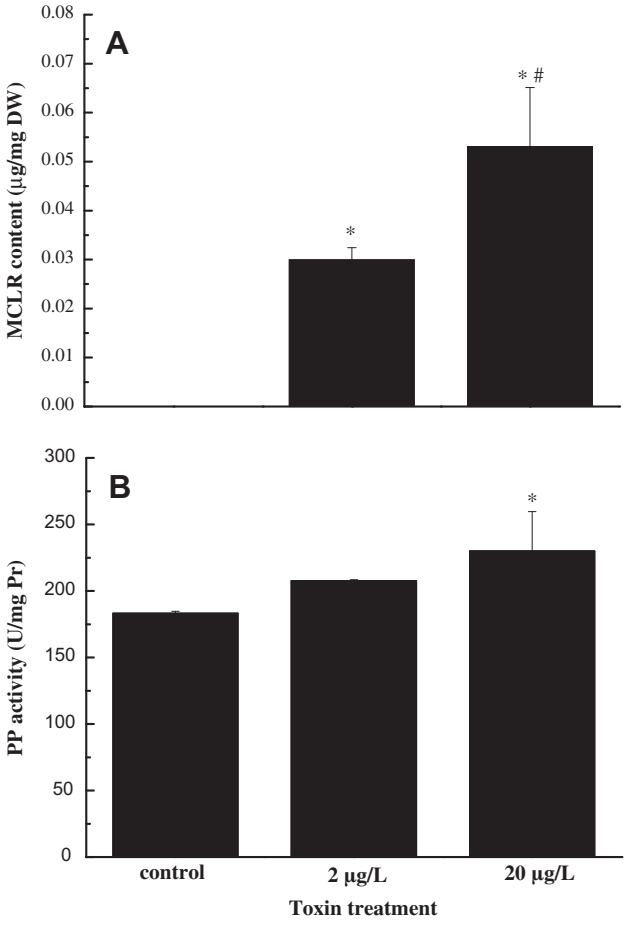

Fig. 1. MCLR contents (A) and PP activity (B) in the brains of the zebrafish *Danio rerio* after 30 d of MCLR exposure (control, 2 and 20 μg L^{-1}). Data are expressed as mean values ± SD ($n = 3–4$). Symbol '*' indicates a significant difference at $P < 0.05$ between the control and treatments, while '#' represents a significant difference between the 2 and 20 μg L^{-1} toxin treatments at $P < 0.05$.

3.2. Protein profile in the zebrafish brain exposed to MCLR

The representative 2-DE gels of MCLR exposed and non-exposed zebrafish brains are shown in Fig. 2, and quantitative spot comparisons were conducted using image analysis software. On average, more than 900 proteins spots were detected in each gel using silver staining and the ImageMaster 2D Elite software. Compared with the 2-DE gels of the control brains, a total of 30 protein spots from the treated group was found to significantly alter in abundance ($\geqslant$2-fold; $P < 0.05$). Among these altered proteins, seven protein spots were newly induced in the exposed treatment (one spot was observed in the 2 μg L^{-1} toxin treatment and seven spots in the 20 μg L^{-1} treatment). In addition, six protein spots were significantly downregulated and four protein spots were noticeably upregulated in the 2 μg L^{-1} treatment (Table 1; Fig. 2). In the 20 μg L^{-1} group, twelve protein spots were remarkably downregulated and seven protein spots were markedly upregulated (Table 1; Fig. 2). These altered proteins were excised and submitted for identification using MALDI-TOF/TOF MS analysis. All of the protein spots were successfully identified with CI values greater than 95% (Table 1) and the matched proteins came from the NCBI database for the zebrafish *D. rerio*. The identified proteins were distinguished into 26 different proteins. Of them, four proteins (spots 2, 3, 4 and 17) were involved in cytoskeleton organization, and six proteins (spots 10, 11, 12, 20, 21 and 28) were related to metabolism. Two proteins (spots 14 and 15) were related to the oxidative stress response, and five proteins (spots 5, 6, 9, 22 and 23) played a role in signal transduction. The abundance of PP type 2C alpha 2 (PP2Cα2) was noticeably increased in the 20 μg L^{-1} treatment. The other proteins were found to be correlated with transport, protein degradation, apoptosis and translation. It should be noted that five protein spots (spots 19, 25, 27, 29, and 30) were definitely identified as the same protein (i.e. vitellogenin 1), although these spots were differentially distributed in the 2-DE gel (Fig. 2C).

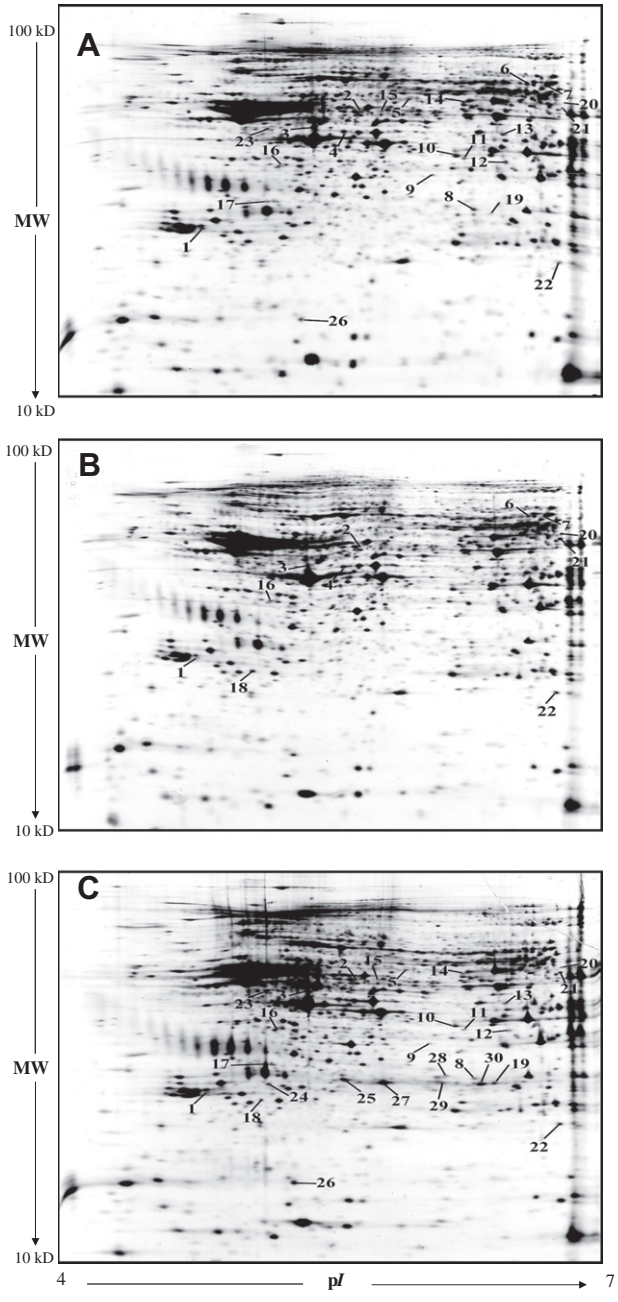

Fig. 2. Representative 2-DE gels of brain proteins in the zebrafish *Danio rerio* after the 30 d MCLR exposure. A: control, B: 2 μg L^{-1}, and C: 20 μg L^{-1}. Whole soluble proteins from zebrafish brains were separated with 2-DE and visualized using silver staining. The protein spots altered by MCLR exposure are labeled with numbers. The molecular weights (MW) and p*I* scales are indicated. Each gel is representative of three independent replicates.

4. Discussion

There have been many studies on the toxic effects of MCLR on aquatic organisms and human beings, but little effort has been devoted to exploring the neurotoxicity of MCLR. This study is the first effort to investigate the biochemical mechanism involved in the chronic neurotoxicity of MCs on fish brain at the proteomic level, although MCs probably appear to have presented neurotoxicity in several previous studies (Cazenave et al., 2005, 2008; Fischer et al., 2005; Soares et al., 2006; Feurstein et al., 2009). After 30 d exposure, a significant amount of MCLR was detected in the treated group (Fig. 1A). This is in line with a study that a carp (*C. carpio*) treated with a single dose of 400 μg kg^{-1} DW MCLR demonstrates the presence of MCLR in the brain 48 h post toxin application (Fischer and Dietrich, 2000), which allows this toxin to exert its probable neurotoxicity. However, care needs to be taken with MCs content in organisms, since the present organic extraction method can not efficiently extract covalently bound MCs (Williams et al., 1997; Martins and Vasconcelos, 2009). In this study, MCLR was extracted from the zebrafish brain exposed to dissolved MCLR using the same procedure reported by Moreno et al. (2005), which might omit covalently bound MCLR. However, Lance et al. (2010) recently demonstrate the accumulation of covalently bound MCs in *Lymnaea stagnalis* exposed to toxic cyanobacteria, whereas bound MCs are not detected in dissolved MCLR exposed *L. stagnalis*. Overall, the covalently bound MCLR as well as non-covalently bound MCLR should be considered with regard to the toxicological study in future.

Using the proteomic approach, 30 differentially expressed proteins caused by MCLR were identified and these proteins were assigned into several groups such as cytoskeleton, metabolism, oxidative stress, signal transduction, protein degradation, transport, apoptosis and translation related. It is worth emphasizing that the proteomic response in the zebrafish brain was dependent on MCLR concentration. Of 30 differentially expressed protein spots, 11 protein spots were observed in the 2 μg L^{-1} treatment while 27 spots were found in the 20 μg L^{-1} group, which might be caused by a significantly differential toxin accumulation in the zebrafish brain after the exposure to different MCLR concentrations.

This study showed that MCLR treatment produced oxidative stress in the zebrafish brain. Particularly, mitochondrial aldehyde dehydrogenase 2, a target of MCLR attack in a study (Chen et al.,

Table 1
Identification of the differentially expressed proteins in the zebrafish (*Danio rerio*) brain following MCLR exposure.

Spot id.	Accession number	Protein score	Protein score CI%	Peptide count	MW/p*I*	Protein description	Fold change	
							2 μg L^{-1}	20 μg L^{-1}
Cytoskeleton								
2	gi|18858539	280	100	22	54.02/5.50	Desmin	−2.08	−2.65
3	gi|62298523	446	100	13	41.74/5.30	Beta-actin-1	−2.22	−2.38
4	gi|41054750	61	99.111	13	55.98/6.29	Zgc:66419	−2.53	–
17	gi|47086499	116	100	5	27.48/5.08	Tubulin folding cofactor B	–	3.40
Metabolism								
10	gi|48734808	275	100	14	40.31/6.73	NADH dehydrogenase [ubiquinone] 1 alpha subcomplex subunit 10	–	−2.12
11	gi|41054629	56	97.057	4	30.83/5.99	Methylthioadenosine phosphorylase	–	−2.06
12	gi|33468556	136	100	4	35.11/6.25	Novel protein similar to human glyoxylate reductase/hydroxypyruvate reductase	–	−2.12
20	gi|47086189	62	99.243	14	60.75/7.54	Propionyl-CoA carboxylase, beta polypeptide	5.97	2.15
21	gi|55925442	164	100	10	57.17/8.46	3-oxoacid CoA transferase 1a	3.97	2.12
28	gi|41055658	54	95.745	7	34.59/8.35	3-hydroxyisobutyrate dehydrogenase b	–	N[a]
Oxidative stress response								
14	gi|41393103	302	100	13	55.23/6.18	Aldehyde dehydrogenase 9A1a	–	−2.09
15	gi|41053732	120	100	7	56.53/5.93	Aldehyde dehydrogenase 2 family (Mitochondrial) a	–	−2.19
Signal transduction								
5	gi|41055564	90	99.999	9	59.12/5.67	Copine I	–	−2.97
6	gi|71164796	326	100	15	53.53/6.39	Synaptic vesicle membrane protein VAT-1 homolog	−3.10	–
9	gi|61806564	63	99.399	6	37.33/5.61	Guanine nucleotide binding protein (G protein), beta polypeptide 2	–	−2.10
22	gi|54312133	105	100	6	20.85/6.31	phosphatidylethanolamine binding protein	2.56	2.43
23	gi|47271364	145	100	8	42.06/5.18	protein phosphatase type 2C alpha 2	–	2.23
Transport								
7	gi|47264590	414	100	25	73.48/6.81	TPA:TPA_exp: transferrin	−4.39	–
8	gi|47777306	89	99.998	8	30.61/6.23	Voltage-dependent anion channel 1	–	−2.10
24	gi|11118642	106	100	9	139.51/6.92	Vitellogenin 3	–	N[a]
25	gi|166795887	288	100	16	149.45/8.68	Vitellogenin 1	–	N[a]
27	gi|166795887	546	100	18	149.45/8.68	Vitellogenin 1	–	N[a]
29	gi|166795887	107	100	11	149.45/8.68	Vitellogenin 1	–	N[a]
30	gi|166795887	75	99.962	11	149.45/8.68	Vitellogenin 1	–	N[a]
19	gi|166795887	72	99.929	11	149.45/8.68	Vitellogenin 1	–	3.18
Protein degradation								
13	gi|45709356	55	96.12	12	55.98/8.16	Sb:cb283 protein	–	−2.58
16	gi|47085817	165	100	11	37.57/5.11	Ubiquitin carboxyl-terminal hydrolase L5	3.28	2.55
18	gi|41393111	160	100	5	24.23/5.10	Ubiquitin carboxyl-terminal esterase L1	N[a]	N[a]
Apoptosis								
1	gi|47938859	220	100	14	27.94/4.78	Ywhai protein	−3.03	−3.86
Translation								
26	gi|47085971	114	100	3	16.87/5.18	Eukaryotic translation initiation factor 5A	–	2.43

MW: molecular weight. p*I*: isoelectric point.
Note: variations were calculated as treated/control spot volume ratio and if the result was below 1, it is reported as – control/treated ratio.
[a] These proteins are newly induced in the treated group.

2006), presented a significant decrease in abundance under toxin treatment. Similarly, the expression of aldehyde dehydrogenase 9A1a was significantly depressed by MCLR. Aldehyde dehydrogenases are known to participate in aldehyde metabolism via oxidizing aldehyde to carboxylic acid (Marchitti et al., 2007). Aldehydes are highly reactive and cytotoxic, and are involved in various physiological processes such as enzyme inactivation, protein modification, and DNA damage (Lindahl, 1992; O'Brien et al., 2005). Moreover, increasing evidence suggests that some aldehyde metabolites (e.g. 3,4-dihydroxyphenylacetaldehyde and 3,4-dihydroxyphenylglycoladehyde) are neurotoxic, and their intraneuronal accumulation has been regarded as one mechanism that might be involved in cell death associated with neurodegenerative conditions, including Parkinson's disease and Alzheimer's disease (Mattammal et al., 1995; Burke et al., 2003). Thus, MCLR treatment caused an accumulation of aldehyde via a strong inhibition of aldehyde dehydrogenases and subsequently resulted in oxidative stress (i.e. lipid peroxidation, GSH depletion and reduced antioxidant activity), indicating that MCLR caused neurotoxicity in zebrafish.

MCLR also caused cytoskeletal disruption in the brain, which is consistent with several previous studies (Mezhoud et al., 2008a,b; Malécot et al., 2009; Wang et al., 2010). Desmin is the major muscle-specific intermediate filament protein, and its mutations cause severe forms of myofibrillar myopathy characterized by partial aggregation of extrasarcomeric desmin cytoskeleton and structural disorganization of myofibrils (Kreplak and Bär, 2009). β-actin is a major cytoskeletal protein composed of actin filaments, which are abundant in synaptic areas such as pre-synaptic nerve endings and post-synaptic dendrites (Ratner and Mahler, 1983; Toh et al., 1976), where they exist as a submembranous cytoskeleton and are involved in neurite growth, cell adhesion, synapse formation, and exocytosis of neurotransmitters (Sobue and Kanda, 1989; Asanuma et al., 1993). A study shows that β-actin mRNAs are strikingly decreased in the gerbil brain after transient ischemia, which might be attributable to neuronal death (Asanuma et al., 1993). A decreased β-actin expression might be caused by oxidative stress due to MCLR attack, since actin could be a direct target for oxidative modification (Fiaschi et al., 2006; Lassing et al., 2007). Tubulin folding cofactor B is a ubiquitously expressed tubulin chaperone protein and binds to α-tubulin (Wang et al., 2005), and its substantial accumulation leads to microtubule depolymerization, growth cone retraction, and axonal damage followed by neuronal degeneration (Lopez-Fanarraga et al., 2007). Therefore, the variations of cytoskeletal proteins indicated that MCLR caused cellular damage in the brain due to cytoskeletal disruptions.

Our study demonstrated that MCLR treatment exerted a significant effect on signal transduction. The first affected protein was copine I, which belongs to the copine family, a family of Ca^{2+}-dependent and phospholipid-binding proteins. The copines comprise a pathway for calcium signaling to proteins involved in a wide range of biological activities including growth control, exocytosis, mitosis, apoptosis, gene transcription, and cytoskeleton assembly. Especially, it has been reported that copine I plays a role in regulating the TNF-α signaling pathway (Tomsig et al., 2004). VAT-1, which was first described in the electric organs of the Pacific electric ray *Torpedo californica*, is a vital component of synaptic vesicle formation (Linial et al., 1989) and therefore involved in nerve function and communication. The heterotrimeric guanine nucleotide binding protein (G protein) is composed of three subunits, Gα, Gβ and Gγ, and each of them has many isoforms (Cabrera-Vera et al., 2003). Gβ2 (guanine nucleotide binding protein, beta polypeptide 2) is widely expressed throughout the brain (Betty et al., 1998). A study demonstrates that Gβ2 directly interacts with neuropathy target esterase (NTE), and the silence of Gβ2 inhibits the activity of NTE (Chen et al., 2007). The specific deletion of NTE could cause neurodegeneration in animals (Akassoglou et al., 2004; Muhlig-Versen et al., 2005). The phosphatidylethanolamine binding protein (PEBP) is known to be a Raf kinase inhibitor protein and it mainly functions as a direct negative regulator of signaling kinase such as mitogen-activated protein kinase (MAPK), G protein-coupled receptor kinase, nuclear factor kappa B signaling cascades, and also serine proteases (Yeung et al., 1999). Overall, the toxin-induced deregulation in signal transduction was supposed to be an indirect evidence of neurotoxicity in the zebrafish brain due to MCLR attack.

The most interesting finding of this study is that MCLR enhanced the expression of PP2Cα2. The PP activity also increased with an increasing MCLR concentration in our study, which was inconsistent with previous studies (Guzman et al., 2003; Malbrouck et al., 2003, 2004). Guzman et al. (2003) show that a lethal dose of MCLR profoundly inhibits PP activity in the nuclear compartment. Nevertheless, our previous work on the zebrafish liver demonstrates an increased hepatic PP activity under MCLR treatment (Wang et al., 2010). Additionally, a previous study shows that MCRR can up-regulate the expression of the PP2A A subunit in human amniotic epithelial cells (Fu et al., 2009). In this study, an upregulation of PP2Cα2 might be responsible for an increased PP activity in the treated brain. The highly conserved PP2C family is one of four major groups of serine/threonine PPs in eukaryotes (Cohen, 1989), and it is involved in various cellular events and signaling pathways. For example, an overexpression of PP2Cα leads to G_2/M cell cycle arrest and apoptosis through activation of the p53 protein kinase pathway (Ofek et al., 2003). Also, PP2C is involved in the regulation of AMP-activated protein kinase (AMPK) (Moore et al., 1991) and the stress-activated protein kinase pathway (Hanada et al., 1998, 2001). Thus, an overexpression of PP2Cα2 might affect the protein kinase signaling pathway (e.g. MAPK and AMPK), which should deepen our understanding about the toxicological mechanism of MCLR. Alternatively, the increased expression of PP2Cα2 might merely be a compensatory effect of the cells in fighting against toxin attack, which really deserves further investigation.

Our study showed that several proteins involved in transporting were affected by MCLR. Transferrin is one of the major serum proteins in eukaryotes and plays a crucial role in iron metabolism by binding and transporting iron, thus making it unavailable for catalysis of superoxide radical formation via Fenton reactions (Neves et al., 2009). A depressed transferrin abundance in this study might be correlated with the toxin-induced oxidative stress, for its decrease making iron available for catalysis of the superoxide radical formation. The voltage-dependent anion channel (VDAC) is instrumental in the release of calcium, cytochrome c and apoptosis inducing factor from the mitochondria inner membrane space, thus enabling the mitochondria to control cell death (Crompton, 1999; Tsujimoto and Shimizu, 2002). The VDAC protein is also a determinant of necrosis (Crompton, 1999). Thus, a decreased VDAC expression could be considered to be aimed at reducing cell death. Interestingly, MCLR induced the expression of vitellogenin 3 and significantly increased the abundance of vitellogenin 1 in zebrafish brains. It should be noted that spots 19, 25, 27, 29, and 30 were identified as the same protein (vitellogenin 1), and these proteins are likely to be protein isoforms. Protein isoforms can arise from alternative mRNA splicing and various post-translational modifications, such as cleavage, phosphorylation, acetylation, and glycosylation. Although vitellogenin (Vg) is mostly distributed in fish liver, it could be expressed in other tissues (e.g. heart and brain) (Ma et al., 2009). Considering that Vg induction is used as a biomarker of exposure of fish to estrogen-active substances (Andersen et al., 2006), we speculated that MCLR might mimic the effects of endocrine disrupting chemicals (EDCs), due to this toxin treatment significantly increasing Vg expression. In fact, the estrogenic activity

of this toxin has recently been exemplified by a study which clearly indicates that MCLR presents estrogenic potential likely by indirect interaction with estrogen receptors (Oziol and Bouaïcha, 2010).

Meanwhile, MCLR treatment affected protein degradation in zebrafish brains. Sb:cb283 protein with aminopeptidase activity is involved in proteolysis. Then, MCLR affected proteolysis in organism, which is consistent with our previous study (Wang et al., 2010). Ubiquitin carboxyl-terminal hydrolase L5 and ubiquitin carboxyl-terminal esterase L1 are involved in the ubiquitin proteasome system, a cellular pathway responsible for the degradation of misfolded and damaged proteins (Ciechanover and Brundin, 2003). These proteins may collaborate to affect the turnover of cellular proteins (e.g. misfolded and damaged proteins) when cells were stressed by MCLR. Therefore, our study presented a new clue to understanding the molecular mechanisms underlying MCLR-induced cellular responses.

Brain metabolism is known to be disturbed by MCLR treatment. NADH [ubiquinone] dehydrogenase 1 alpha subcomplex subunit 10 (NDUFA10) is a subunit of NADH ubiquinone oxidoreductase (complex I of the respiratory chain, Talpade et al., 2000), and is involved in energy metabolism. Recent studies suggest that complex I is a potent source of ROS (Murphy, 2009), and the decrease of NDUFA10 abundance might decrease energy production from the respiratory chain, however, concomitantly releasing the brain from oxidative attack via decreasing ROS production. Propionyl-CoA carboxylase is involved in the catabolism of essential amino acids, odd-chain fatty acids, and side chains of cholesterol (Muro et al., 2001). 3-oxoacid CoA transferase transfers the CoA residue from succinyl-CoA to acetoacetate to form acetoacetyl-CoA as a mitochondrial energy source (Tildon and Sevdalian, 1972). 3-hydroxyisobutyrate dehydrogenase participates in valine, leucine and isoleucine degradation for the generation of energy (Robinson and Coon, 1957). Then, an overexpression of propionyl-CoA carboxylase, beta polypeptide and 3-oxoacid CoA transferase 1a, and a newly induced 3-hydroxyisobutyrate dehydrogenase b increased energy requirement in the treated brain, and was supposed to be a compensatory mechanism in facing the decreasing energy produced due to the oxidative stress under MCLR treatment. Methylthioadenosine phosphorylase (MTAP) is a key enzyme in purine biosynthesis and the methionine salvage pathway. MTAP is usually abundant in normal tissues, but is known to be deficient in a variety of cancers (Barker et al., 1997; Chen et al., 1996). Human glyoxylate reductase/hydroxypyruvate reductase plays a critical role in the removal of the metabolic by-product glyoxylate from the liver. Deficiency of this enzyme is the underlying cause of primary hyperoxaluria type 2 and leads to increased urinary oxalate levels, formation of kidney stones and renal failure (Booth et al., 2006). Overall, MCLR might cause a dysfunction in the zebrafish brain via disturbing energy generation and organic acid metabolism.

MCLR could cause apoptosis in the brain, since toxin treatment significantly reduced the abundance of Ywhai protein (belonging to the 14-3-3 family). This 14-3-3 protein is a phosphoserine specific adapter protein, which can bind the phosphorylated Bad protein and so prevent apoptosis (Akassoglou et al., 2004; Muslin et al., 1996). Here, the downregulation of Ywhai protein might lead to cytoplasmic release of phosphorylated Bad protein and induce pro-apoptotic activity. A study shows that global disruption of 14-3-3 function results in premature cell cycle entry, release of G1 cells from interphase arrest and loss of the S-phase check point after DNA damage, accompanied by high levels of cell death (Nguyen et al., 2004). Eukaryotic translation initiation factor 5A (eIF5A) is identified as the unique hypusine-containing protein (Park et al., 1981), and it participates in the translational process (Jao and Chen, 2006). Recent studies indicate that eIF5A may also play a role in cell death (Li et al., 2004; Taylor et al., 2004). For instance, an overexpression of eIF5A has been found to induce apoptosis in lung cancer cells (Li et al., 2004). Thus, the increase of eIF5A abundance indicated that MCLR resulted in a toxin-inducing apoptosis in the treated brain.

5. Conclusions

Our study provided a new insight into MCLR neurotoxicity in zebrafish brains at the proteomic level. The proteomic analysis

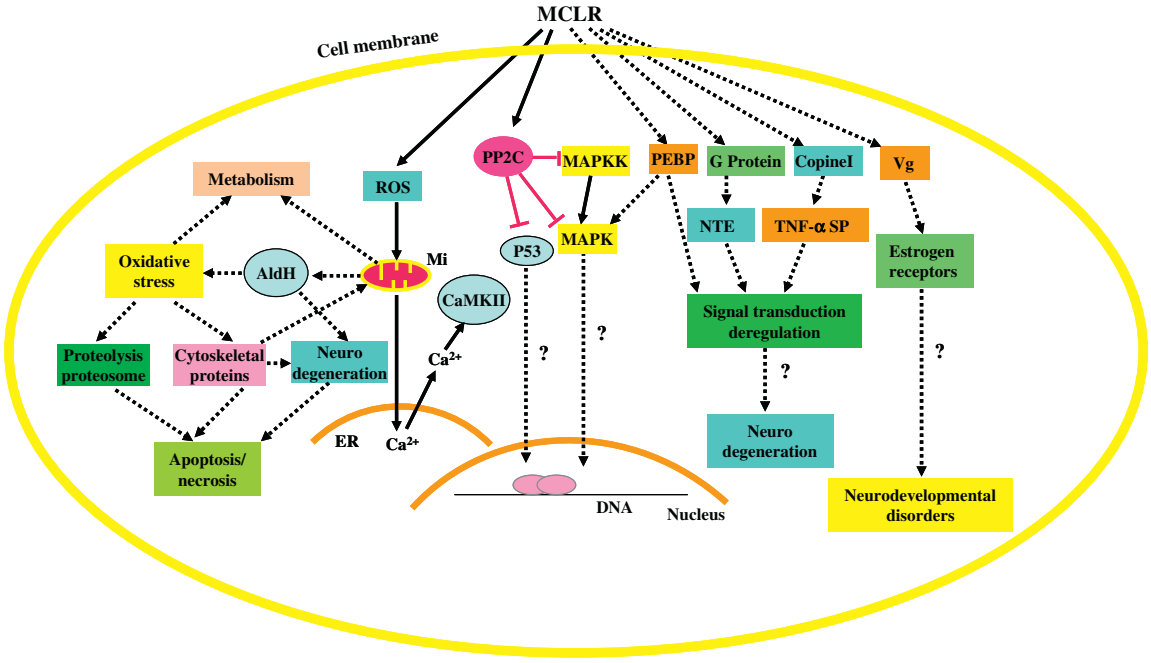

Fig. 3. The proposed scheme illustrating cellular events in zebrafish brains upon microcystin-LR (MCLR) exposure. AldH: aldehyde dehydrogenase; CaMKII: calcium/calmodulin-dependent kinase; ER: endoplasmic reticulum; MAPK: mitogen-activated kinase; MAPKK: mitogen-activated kinase kinase; MCLR: microcystin-LR; Mi: mitochondria; NTE: neuropathy target esterase; PEBP: phosphatidylethanolamine binding protein; PP2C: protein phosphatase 2C; ROS: reactive oxygen species; TNF-α SP: TNF-α signaling pathway; Vg: vitellogenin.

revealed that MCLR neurotoxicity induced oxidative stress, and a dysfunction of cytoskeleton assembly and macromolecule metabolism, with a concomitant interference with signal transduction and other functions (e.g. protein degradation, transport, apoptosis and translation), suggesting that MCLR toxicity to the zebrafish brain was complex and diverse (Fig. 3). Also, the PP activity in the brain was enhanced with an increasing MCLR concentration, and this was partly exemplified by an overexpression of PP2Cα2 under toxin treatment. Thus, our study firstly demonstrated that the chronic neurotoxicity of MCLR might initiate the PP pathway via an upregulation of PP2C in the zebrafish brain, in addition to the ROS pathway. In addition an increased Vg expression in the treated group suggested that MCLR might mimic the effects of EDCs, and this really deserves further study. It should be noted that the responses in brain were different from liver in our earlier study (Wang et al., 2010), i.e. MCLR specifically affected transport, protein degradation, apoptosis and translation in zebrafish brains. Moreover, even though the affected cellular processes were overlapped in general functional categories (e.g. metabolism, cytoskeletonal assembly, oxidative stress and signal transduction), none of the proteins in the functional category in brain was the same as that from liver.

Acknowledgements

This work was partially supported by the National Natural Science Foundation of China (No. 40806051), the State Key Laboratory of Marine Environmental Science, and the Program for New Century Excellent Talents in University to Prof. D.-Z. Wang. The authors thank Prof. John Hodgkiss for helping to revise the manuscript.

References

Asanuma, M., Ogawa, N., Hirata, H., Chou, H., Kondo, Y., Mori, A., 1993. Ischemia-induced changes in α-tubulin and β-actin mRNA in the gerbil brain and effects of bifemelane hydrochloride. Brain Res. 600, 243–248.

Akassoglou, K., Malester, B., Xu, J., Tessarollo, L., Rosenbluth, J., Chao, M.V., 2004. Brain-specific deletion of neuropathy target esterase/swisscheese results in neurodegeneration. Proc. Natl. Acad. Sci. U.S.A. 101, 5075–5080.

Andersen, L., Goto-Kazeto, R., Trant, J.M., Nash, J.P., Korsgaard, B., Bjerregaard, P., 2006. Short-term exposure to low concentrations of the synthetic androgen methyltestostrone affects vitellogenin and steroid levels in adult male zebrafish (*Danio rerio*). Aquat. Toxicol. 76, 343–352.

Baganz, D., Staaks, G., Pflugmacher, S., Steinberg, C.E.W., 2004. A comparative study on microcystin-LR induced behavioural changes of two fish species (*Danio rerio* and *Leucaspius delineatus*). Environ. Toxicol. 19, 564–570.

Barker, F.G., Chen, P., Furman, F., Aldape, K.D., Edwards, M.S., Israel, M.A., 1997. P16 deletion and mutation analysis in human brain tumors. J. Neurooncol. 31, 17–23.

Batista, T., de Sousa, G., Suput, J.S., Rahmani, R., Suput, D., 2003. Microcystin-LR causes the collapse of actin filaments in primary human hepatocytes. Aquat. Toxicol. 65, 85–91.

Betty, M., Harnish, S.W., Rhodes, K.J., Cockett, M.I., 1998. Distribution of heterotrimeric G-protein beta and gamma subunits in the rat brain. Neuroscience 85, 475–486.

Blom, J.F., Jüttner, F., 2005. High crustacean toxicity of microcystin congeners does not correlate with high protein phosphatase inhibitory activity. Toxicon 46, 465–470.

Booth, M.P.S., Conners, R., Rumsby, G., Brady, R.L., 2006. Structural basis of substrate specificity in human glyoxylate reductase/hydroxypyruvate reductase. J. Mol. Biol. 360, 178–189.

Burke, W.J., Li, S.W., Williams, E.A., Nonneman, R., Zahm, D.S., 2003. 3,4-Dihydroxyphenylacetaldehyde is the toxic dopamine metabolite in vivo: implications for Parkinson's disease pathogenesis. Brain Res. 989, 205–213.

Cabrera-Vera, T.M., Vanhauwe, J., Thomas, T.O., Medkova, M., Preininger, A., Mazzoni, M.R., Hamm, H.E., 2003. Insights into G protein structure, function, and regulation. Endocr. Rev. 24, 765–781.

Carmichael, W.W., Azevedo, S.M., An, J.S., Molica, R.J., Jochimsen, E.M., Lau, S., Rinehart, K.L., Shaw, G.R., Eaglesham, G.K., 2001. Human fatalities from cyanobacteria: chemical and biological evidence for cyanotoxins. Environ. Health Perspect. 109, 663–668.

Cazenave, J., Wunderlin, D.A., Bistoni, M.A., Amé, M.V., Krause, E., Pflugmacher, S., Wiegand, C., 2005. Uptake, tissue distribution and accumulation of microcystin-RR in *Corydoras paleatus*, *Jenynsia multidentata* and *Odontesthes bonariensis*. A field and laboratory study. Aquat. Toxicol. 75, 178–190.

Cazenave, J., Nores, M.L., Miceli, M., Díaz, M.P., Wunderlin, D.A., Bistoni, M.A., 2008. Changes in the swimming activity and the glutathione-S-transferase activity of *Jenynsia multidentata* fed with microcystin-RR. Water Res. 42, 1299–1307.

Chen, Z.H., Zhang, H., Savarese, T.M., 1996. Gene deletion chemoselectivity: codeletion of the genes for p16 (INK4), methylthioadenosine phosphorylase, and the alpha and beta-interferons in human pancreatic cell carcinoma lines and its implications for chemotherapy. Cancer Res. 56, 1083–1090.

Chen, T., Cui, J., Liang, Y., Xin, X.B., Young, D.O., Chen, C., Shen, P.P., 2006. Identification of human liver mitochondrial aldehyde dehydrogenase as a potential target for microcystin-LR. Toxicology 220, 71–80.

Chen, R., Chang, P.-A., Long, D.-X., Liu, C.-Y., Yang, L., Wu, Y.-J., 2007. G protein β2 subunit interacts directly with neuropathy target esterase and regulates its activity. Int. J. Biochem. Cell Biol. 39, 124–132.

Ciechanover, A., Brundin, P., 2003. The ubiquitin proteasome system in neurodegenerative diseases: sometimes the chicken, sometimes the egg. Neuron 40 (2), 427–446.

Cohen, P., 1989. The structure and regulation of protein phosphatases. Annu. Rev. Biochem. 58, 453–508.

Crompton, M., 1999. The mitochondrial permeability transition pore and its role in cell death. Biochem. J. 341, 233–349.

Deblois, C.P., Aranda-Rodriguez, R., Giani, A., Bird, D.F., 2008. Microcystin accumulation in liver and muscle of tilapia in two large Brazilian hydroelectric reservoirs. Toxicon 51, 435–448.

Ding, W.X., Shen, H.M., Ong, C.N., 2001. Critical role of reactive oxygen species formation in microcystin-induced cytoskeleton disruption in primary cultured hepatocytes. J. Toxicol. Environ. Health 64, 507–519.

Feurstein, D., Holst, K., Fischer, A., Dietrich, D.R., 2009. Oatp-associated uptake and toxicity of microcystins in primary murine whole brain cells. Toxicol. Appl. Pharmacol. 234, 247–255.

Fiaschi, T., Cozzi, G., Raugei, G., Formigli, L., Ramponi, G., Chiarugi, P., 2006. Redox regulation of beta-actin during integrin-mediated cell adhesion. J. Biol. Chem. 281, 22983–22991.

Fischer, W.J., Dietrich, D.R., 2000. Pathological and biochemical characterization of microcystin-induced hepatopancreas and kidney damage in carp (*Cyprinus carpio*). Toxicol. Appl. Pharmacol. 164, 73–81.

Fischer, W.J., Altheimer, S., Cattori, V., Meier, P.J., Dietrich, D.R., Hagenbuch, B., 2005. Organic anion transporting polypeptides expressed in liver and brain mediate uptake of microcystin. Toxicol. Appl. Pharmacol. 203, 257–263.

Fontal, O.I., Vieytes, M.R., Baptista de Sousa, J.M., Louzao, M.C., Botana, L.M., 1999. A fluorescent microplate assay for microcystin-LR. Anal. Biochem. 269, 289–296.

Fu, W., Yu, Y., Xu, L., 2009. Identification of temporal differentially expressed protein responses to microcystin in human amniotic epithelial cells. Chem. Res. Toxicol. 22, 41–51.

Gehringer, M.M., 2004. Microcystin-LR and okadaic acid-induced cellular effects: a dualistic response. FEBS Lett. 557, 1–8.

Gurbuz, F., Metcalf, J.S., Karahan, A.G., Codd, G.A., 2009. Analysis of dissolved microcystins in surface water samples from Kovada Lake, Turkey. Sci. Total Environ. 407, 4038–4046.

Guzman, R.E., Solter, P.F., Runnegar, M.T., 2003. Inhibition of nuclear protein phosphatase activity in mouse hepatocytes by the cyanobacterial toxin microcystin-LR. Toxicon 41, 773–781.

Hagenbuch, B., Meier, P.J., 2003. The superfamily of organic anion transporting polypeptides. Biochim. Biophys. Acta 1609, 1–18.

Hanada, M., Kobayashi, T., Ohnishi, M., Ikeda, S., Wang, H., Katsura, K., Yanagawa, Y., Hiraga, A., Kanamaru, R., Tamura, S., 1998. Selective suppression of stress-activated protein kinase pathway by protein phosphatase 2C in mammalian cells. FEBS Lett. 437, 172–176.

Hanada, M., Ninomiya-Tsuji, J., Komaki, K., Ohnishi, M., Katsura, K., Kanamaru, R., Matsumoto, K., Tamura, S., 2001. Regulation of the TAK1 signaling pathway by protein phosphatase 2C. J. Biol. Chem. 276, 5753–5759.

Hoeger, S.J., Hitzfeld, B.C., Dietrich, D.R., 2005. Occurrence and elimination of cyanobacterial toxins in drinking water treatment plants. Toxicol. Appl. Pharmacol. 203, 231–242.

Jao, D.L., Chen, K.Y., 2006. Tandem affinity purification revealed the hypusine-dependent binding of eukaryotic initiation factor 5A to the translating 80S ribosomal complex. J. Cell. Biochem. 97, 583–598.

Kreplak, L., Bär, H., 2009. Severe myopathy mutations modify the nanomechanics of desmin intermediate filaments. J. Mol. Biol. 385, 1043–1051.

Lance, E., Neffling, M.R., Gérard, C., Meriluoto, J., Bormans, M., 2010. Accumulation of free and covalently bound microcystins in tissues of *Lymnaea stagnalis* (Gastropoda) following toxic cyanobacteria or dissolved microcystin-LR exposure. Environ. Pollut. 158, 674–680.

Lassing, I., Schmitzberger, F., Björnstedt, M., Holmgren, A., Nordlund, P., Schutt, C.E., Lindberg, U., 2007. Molecular and structural basis for redox regulation of β-actin. J. Mol. Biol. 370, 331–348.

Li, A., Li, H.-Y., Jin, B.-F., Ye, Q.-N., Zhou, T., Yu, X.-D., Pan, X., Man, J.-H., He, K., Yu, M., Hu, M.R., Wang, J., Yang, S.C., Shen, B.F., Zhang, X.M., 2004. A novel eIF5A complex functions as a regulator of p53 and p53-dependent apoptosis. J. Biol. Chem. 279, 49251–49258.

Li, L., Xie, P., Li, S.X., Qiu, T., Guo, L.G., 2007. Sequential ultrastructural and biochemical changes induced *in vivo* by the hepatotoxic microcystins in liver of the phytoplanktivorous silver carp *Hypophthalmichthys molitrix*. Comp. Biochem. Physiol. C: Pharmacol. Toxicol. 146, 357–367.

Lindahl, R., 1992. Aldehyde dehydrogenases and their role in carcinogensis. Crit. Rev. Biochem. Mol. Biol. 27, 283–335.

Linial, M., Miller, K., Scheller, R.H., 1989. VAT-1: an abundant membrane protein from Torpedo cholinergic synaptic vesicles. Neuron 2, 1265–1273.
Lopez-Fanarraga, M., Carranza, G., Bellido, J., Kortazar, D., Villegas, J.C., Zabala, J.C., 2007. Tubulin cofactor B plays a role in the neuronal growth cone. J. Neurochem. 100, 1680–1687.
Ma, L., Li, D., Wang, J., He, J., Yin, Z., 2009. Effects of adrenergic agonists on the extrahepatic expression of vitellogenin Ao1 in heart and brain of the Chinese rare minnow (*Gobiocypris rarus*). Aquat. Toxicol. 91, 19–25.
Malbrouck, C., Trausch, G., Devos, P., Kestemont, P., 2003. Hepatic accumulation and effects of microcystin-LR on juvenile goldfish *Carassius auratus* L. Comp. Biochem. Physiol. C: Toxicol. Pharmacol. 135, 39–48.
Malbrouck, C., Trausch, G., Devos, P., Kestemont, P., 2004. Effect of microcystin-LR on protein phosphatase activity and glycogen content in isolated hepatocytes of fed and fasted juvenile goldfish *Carassius auratus* L. Toxicon 44, 927–932.
Malécot, M., Mezhoud, K., Marie, A., Praseuth, D., Puiseux-Dao, S., Edery, M., 2009. Proteomic study of the effects of microcystin-LR on organelle and membrane proteins in medaka fish liver. Aquat. Toxicol. 94, 153–161.
Marchitti, S.A., Deitrich, R.A., Vasiliou, V., 2007. Neurotoxicity and metabolism of the catecholamine-derived 3,4-dihydroxyphenylacetaldehyde and 3,4-dihydroxyphenylglycolaldehyde: the role of aldehyde dehydrogenase. Pharmacol. Rev. 59, 125–150.
Martins, J.C., Vasconcelos, V.M., 2009. Microcystin dynamics in aquatic organisms. J. Toxicol. Environ. Health Part B 12, 65–82.
Mattammal, M.B., Haring, J.H., Chung, H.D., Raghu, G., Strong, R., 1995. An endogenous dopaminergic neurotoxin: implication for Parkinson's disease. Neurodegeneration 4, 271–281.
Mezhoud, K., Bauchet, A.L., Château-Joubert, S., Praseuth, D., Marie, A., François, J.C., Fontaine, J.J., Jaeg, J.P., Cravedi, J.P., Puiseux-Dao, S., Edery, M., 2008a. Proteomic and phosphoproteomic analysis of cellular responses in medaka fish (*Oryzias latipes*) following oral gavage with microcystin-LR. Toxicon 51, 1431–1439.
Mezhoud, K., Praseuth, D., Puiseux-Dao, S., François, J.C., Bernard, C., Edery, M., 2008b. Global quantitative analysis of protein expression and phosphorylation status in the liver of the medaka fish (*Oryzias latipes*) exposed to microcystin-LR I. Balneation study. Aquat. Toxicol. 86, 166–175.
Mikhailov, A., Härmälä-Braskén, A.S., Hellman, J., Meriluoto, J., Eriksson, J.E., 2003. Identification of ATP-synthase as a novel intracellular target for microcystin-LR. Chem. Biol. Interact. 142, 223–237.
Monks, N.R., Liu, S., Xu, Y., Yu, H., Bendelow, A.S., Moscow, J.A., 2007. Potent toxicity of the phosphatase inhibitor microcystin LR and microcystin analogues in OATPB1- and OATP1B3-expressing HeLa cells. Mol. Cancer Ther. 6, 587–598.
Moore, F., Weekes, J., Hardie, D.G., 1991. Evidence that AMP triggers phosphorylation as well as direct allosteric activation of rat liver AMP-activated protein kinase. A sensitive mechanism to protect the cell against ATP depletion. Eur. J. Biochem. 199, 691–697.
Moreno, I.M., Molina, R., Jos, A., Picó, Y., Cameán, A.M., 2005. Determination of microcystins in fish by solvent extraction and liquid chromatography. J. Chromatogr. A 1080, 199–203.
Muhlig-Versen, M., da Cruz, A.B., Tschape, J.A., Moser, M., Buttner, R., Athenstaedt, K., Glynn, P., Kretzschmar, D., 2005. Loss of Swiss cheese/neuropathy target esterase activity causes disruption of phosphatidylcholine homeostasis and neuronal and glial death in adult *Drosophila*. J. Neurosci. 25, 2865–2873.
Muro, S., Pérez, B., Desviat, L.R., Rodríguez-Pombo, P., Pérez-Cerdá, C., Clavero, S., Ugarte, M., 2001. Effect of *PCCB* gene mutations on the heteromeric and homomeric assembly of propionyl-CoA carboxylase. Mol. Genet. Metab. 74, 476–483.
Murphy, M.P., 2009. How mitochondria produce reactive oxygen species. Biochem. J. 417, 1–13.
Muslin, A.J., Tanner, J.W., Allen, P.M., Shaw, A.S., 1996. Interaction of 14-3-3 with signaling proteins is mediated by the recognition of phosphoserine. Cell 84, 889–897.
Neves, J.V., Wilson, J.M., Rodrigues, P.N.S., 2009. Transferrin and ferritin response to bacterial infection: the role of the liver and brain in fish. Dev. Comp. Immunol. 33, 848–857.
Nguyen, A., Rothman, D.M., Stehn, J., Imperiali, B., Yaffe, M.B., 2004. Caged phosphopeptides reveal a temporal role for 14-3-3 in G1 arrest and S-phase checkpoint function. Nat. Biotechnol. 22, 993–1000.
O'Brien, P.J., Siraki, A.G., Shangari, N., 2005. Aldehyde sources, metabolism, molecular toxicity mechanisms, and possible effects on human health. Crit. Rev. Toxicol. 35, 609–662.
Ofek, P., Ben-Meir, D., Kariv-Inbal, Z., Oren, M., Lavi, S., 2003. Cell cycle regulation and p53 activation by protein phosphatase 2C alpha. J. Biol. Chem. 278, 14299–14305.
Oziol, L., Bouaïcha, N., 2010. First evidence of estrogenic potential of the cyanobacterial heptotoxins the nodularin-R and the microcystin-LR in cultured mammalian cells. J. Hazard. Mater. 174, 610–615.
Park, M.H., Cooper, H.L., Folk, J.E., 1981. Identification of hypusine, an unusual amino acid, in a protein from human lymphocytes and of spermidine as its biosynthetic precursor. Proc. Natl. Acad. Sci. U. S. A. 78, 2869–2873.
Ratner, N., Mahler, H.R., 1983. Structural organization of filamentous proteins in postsynaptic density. Biochemistry 22, 2446–2453.
Robinson, W.G., Coon, M.J., 1957. Purification and properties of beta-hydroxyisobutyric dehydrogenase. J. Biol. Chem. 225, 511–521.
Soares, R.M., Yuan, M., Servaites, J.C., Delgado, A., Magalhaes, V.F., Hilborn, E.D., Carmichael, W.W., Azevedo, S.M., 2006. Sublethal exposure from microcystins to renal insufficiency patients in Rio de Janeiro, Brazil. Environ. Toxicol. 21, 96–103.
Sobue, K., Kanda, K., 1989. Alpha-actinins, calspectrin (brain spectrin or fodrin), and actin participate in adhesion and movement of growth cones. Neuron 3, 311–319.
Song, L.R., Chen, W., Peng, L., Wan, N., Gan, N.Q., Zhang, X.M., 2007. Distribution and bioaccumulation of microcystins in water columns: a systematic investigation into the environmental fate and the risks associated with microcystins in Meiliang Bay, Lake Taihu. Water Res. 41, 2853–2864.
Talpade, D.J., Greene, J.G., Higgins Jr., D.S., Greenamyre, J.T., 2000. In vivo labeling of mitochondrial complex I (NADH:ubiquinone oxidoreductase) in rat brain using [(3)H]dihydrorotenone. J. Neurochem. 75, 2611–2621.
Taylor, C.A., Senchyna, M., Flanagan, J., Joyce, E.M., Cliché, D.O., Boone, A.N., Culp-Stewart, S., Thompson, J.E., 2004. Role of eIF5A in TNF-alpha-mediated apoptosis of lamina cribrosa cells. Invest. Ophthalmol. Visual Sci. 45, 3568–3576.
Tildon, J.T., Sevdalian, D.A., 1972. CoA transferase in the brain and other mammalian tissues. Arch. Biochem. Biophys. 148, 382–390.
Toh, B.H., Gallichio, H.A., Jeffrey, P.L., Livett, B.G., Muller, H.K., Cauchi, M.N., Clarke, F.M., 1976. Anti-actin stains synapses. Nature 264, 648–650.
Tomsig, J.L., Sohma, H., Creutz, C.E., 2004. Calcium-dependent regulation of tumour necrosis factor-alpha receptor signalling by copine. Biochem. J. 378, 1089–1094.
Tsujimoto, Y., Shimizu, S., 2002. The voltage-dependent anion channel: an essential player in apoptosis. Biochemie 84, 187–193.
Wang, W., Ding, J., Allen, E., Zhu, P., Zhang, L., Vogel, H., Yang, Y., 2005. Gigaxonin interacts with tubulin folding cofactor B and controls its degradation through the ubiquitin-proteasome pathway. Curr. Biol. 15, 2050–2055.
Wang, D.Z., Lin, L., Chan, L.L., Hong, H.S., 2009. Comparative studies of four protein preparation methods for proteomic study of the dinoflagellate *Alexandrium* sp. using two-dimensional electrophoresis. Harmful Algae 8, 685–691.
Wang, M., Chan, L.L., Si, M., Hong, H., Wang, D., 2010. Proteomic analysis of hepatic tissue of zebrafish (*Danio rerio*) experimentally exposed to chronic microcystin-LR. Toxicol. Sci. 113, 60–69.
Williams, D.E., Craig, M., Dawe, S.C., Kent, M.L., Holmes, C.F.B., 1997. Evidence for a covalently bound form of microcystin-LR in salmon liver and dungeness crab larvae. Chem. Res. Toxicol. 10, 463–469.
Yeung, K., Seitz, T., Li, S., Janosch, P., McFerran, B., Kaiser, C., Fee, F., Katsanakis, K.D., Rose, D.W., Mischak, H., Sedivy, J.M., Kolch, W., 1999. Suppression of Raf-1 kinase activity and MAP kinase signalling by RKIP. Nature 401, 173–177.